Desalination Investigation using Direst Contact Membrane Distillation

استقصاء تحلية المياه باستخدام غشاء التقطير مباشر الاتصال

Aly M. Elzahaby*, A. Kabeel*, M.M. Basuony and Ayman Refat Abd Elbar
* Tanta University, Faculty of Engineering, Mechanical Power Dept., Egypt.

الملخص

الغرض من هذا البحث هو اجراء تحقيق عملى ونظرى لتحلية المياه المالحة باستخدام غشاء التقطير الأنبوبى مباشر الاتصال. تم دراسة تأثير عوامل التأثير على أداء الوحدة. وتشمل هذه العوامل درجة حرارة دخول ماء التغذية, ومعدل سريان ماء التغذية, وتركيز الأملاح ودرجة حرارة ماء التبريد. يتم أيضا تقييم الكفاءة الحرارية النظام و نسبة الربح الناتج (GOR). وكان مدى التحقيق: درجة حرارة دخول ماء التغذية 70 درجة سيليزية, معدل سريان ماء التغذية من 15 إلى 20 لتر/ الدقيقة, تركيز الأملاح لمياه التغذية من صفر إلى 40 جرام كلوريد الصوديوم لكل لتر من الماء, درجة حرارة دخول ماء التبريد من 20 إلى 56 درجة سيليزية, ومعدل سريان مياه التبريد من 15 إلى 20 لتر/ دقيقة.
الإنتاجية القصوى والكفاءة اليومية، و نسبة الربح الناتج (GOR) من النظام تصل إلى 40.587 كغ / يوم، 64.88%، و0.624 على التوالي. وأخيرا، فقد وجد اتفاق جيد بين النتائج العددية الحالية والنتائج التجريبية.

Abstract

The purpose of the present research is to carry out an experimental and theoretical investigation for salt water desalination using tubular direct contact membrane distillation. The effect of operating parameters on the unit performance was studied. These parameters include feed water inlet temperature, feed water flow rate, salt concentration and cooling water temperature. System thermal efficiency and gain output ratio (GOR) are also evaluated. The investigated range was, 70°C for inlet feed water temperature, from 15 to 20 L/min for feed water flow rate, from 0 to 40 g Nacl/L water for feed water salt concentration, from 20 to 56 °C for the inlet cooling water temperature, and from 15 to 20 L/min for cooling water flow rate.
Maximum productivity, daily efficiency, and Gain output ratio (GOR) of the system reach 40.587 kg/day, 64.88%, and 0.624 respectively. Finally, a good agreement has been found between the present numerical results and experimental results.

1. Introduction

Membrane distillation (MD) is a hybrid process which joins a thermally driven distillation process with a membrane separation process. The pure water is evaporated from saline water by thermal energy and transported through the pores of hydrophobic membrane. The driving force is the vapor pressure difference created by temperature difference across the membrane. Then pure water vapor condensate at the downstream side of the membrane.

The most common configuration of membrane distillation (MD) is direct contact membrane distillation (DCMD) in which heated feed and cold permeate streams are in direct contact with the porous hydrophobic membrane. The difference in the temperature and salt concentration between feed and permeate streams creates the vapor pressure driving force for "DCMD". In addition, the temperature difference plays an important role, where simultaneous heat and mass transfer occur in both the feed, permeate through the porous membrane.

In direct contact membrane distillation, the operation is simple and it requires the least equipment. So, DCMD is the most appropriate configuration for desalination. Therefore DCMD unit is designed, built and used also.

Desalination is the removal of excess salt and minerals from water and it is used to provide pure water from seawater or brackish water.

Desalination of seawater by "DCMD" was investigated by Hote et al [1]. The salt concentration has a little

Received: 9 July, 2015 – Accepted: 20 August, 2015

effect on the permeate flux up to 5% by weight salt, however increasing the feed flow rate in laminar region and temperature difference Between feed side and permeate side have an important effect on the permeate flux. In the present work, the direct contact membrane distillation process is applied to study the desalinating performance of aqueous solution of NaCl, brackish water and seawater. Flux characteristics affected by the process parameters are investigated. Heat and mass transfer are also analyzed in details.

2. Theoretical Study

2.1 Heat Transfer

Membrane distillation is a complicated physical process in which both heat and mass transfer are involved. For heat transfer, heat is first transferred from the heated feed salt solution across the thermal boundary layer to the membrane surface in the form of heat convection. Then the heat passes through the membrane in the form of vapor latent heat and heat conduction. Finally, the heat is removed from the cold –side membrane surface through the boundary layer by convection. The boundary layers next to the membrane may contribute substantially to the overall heat transfer resistance. The heat flux for each step mentioned above can be expressed as follows:

Heat transfer by convection in the feed boundary layer:

$$Q_f = h_f\,(T_f - T_{fm}) \qquad (1)$$

Where h_f is convective heat transfer coefficient in feed side, T_f is bulk feed water temperature and T_{fm} is membrane surface temperature at feed side.

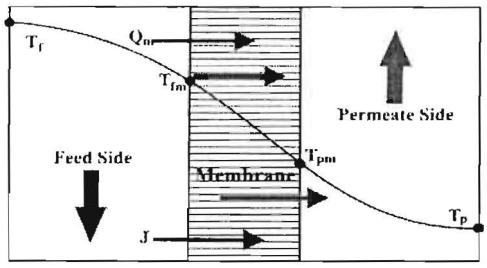

Fig. 1

Fig. 1 The heat transfer process of DCMD

Heat transfer through the membrane by conduction and by movement of vapor across the membrane (latent heat of vaporization):

$$Q_m = Q_{conduction} + Q_{vaporization}$$
$$Q_m = h_m(T_{fm} - T_{pm}) + J.\Delta H_v \qquad (2)$$

Where $h_m = \frac{k_m}{\delta_m}$, h_m is heat transfer coefficient of the membrane, ΔHv is the latent heat of vaporization, δ_m=δ is the thickness of the membrane, J is the molecular flux of water through the membrane and k_m is the thermal conductivity of the membrane:

$$k_m = \varepsilon.k_g + (1-\varepsilon).k_{sm} \qquad (3)$$

Where $k_g$and k_{sm} are the thermal conductivity of air/water vapor and solid membrane material respectively. ε is the porosity of the membrane:

$$\varepsilon = \frac{\text{Avoid volume}}{\text{Total volume of memrane}} \qquad (4)$$

For the permeate side, the convection heat transfer takes place in the permeate boundary layer:

$$Q_p = h_p.(T_{pm} - T_p) \qquad (5)$$

Where h_p is heat transfer coefficient of permeate water, $T_{pm}$is membrane surface temperature at permeate side and T_p is bulk permeate water temperature.

At steady state, the overall heat transfer flux through the membrane is counted and given:

$$Q = Q_f = Q_m = Q_p$$

$$h_f(T_f - T_{fm}) = \frac{k_m}{\delta_m}(T_{fm} - T_{pm}) + J.\Delta H_v = h_p(T_{pm} - T_p) \quad (6)$$

From Eqns. (1) – (6) we obtain the temperature adjacent the membrane for a given flux, in term of the bulk feed and permeate temperatures and the tree heat transfer coefficient:

$$T_{fm} = \frac{h_m\left(T_p + T_f.{}^{h_f}/_{h_p}\right) + h_f.T_f - J.\Delta H_v}{h_m + h_f(1 + {}^{h_m}/_{h_f})} \quad (7)$$

$$T_{pm} = \frac{h_m.\left(T_f + T_p.{}^{h_p}/_{h_f}\right) + h_p.T_p + J.\Delta H_v}{h_m + h_p(1 + {}^{h_m}/_{h_p})} \quad (8)$$

Heat transfer coefficient (h) can be calculated from this equation:

$$h = \frac{Nu*K}{D} \quad (9)$$

Where K is thermal conductivity of water, D is hydraulic diameter of tubular membrane and Nu is Nusselt number of water which can be calculated from the following equations:

For Turbulent flow (Dittus- Boelter equation):

$$Nu = 0.023 * Re^{0.83} * Pr^{0.33} \quad (10)$$

For Laminar flow:

$$Nu = 1.86 * (Re * Pr * {}^{D}/_{L})^{1/3} \quad (11)$$

Where Re is Reynolds number of water, Pr is Prandtl number of water and L is the length of membrane.

2.2 Mass Transfer:

Mass transport across the membrane in DCMD is generally described by various mass transfer models based on the dusty gas model [2], such as the Knudsen model, the Poiseuille model, the Knudsen–Poiseuille transition models, and the molecular diffusion model. The selection of the most appropriate model depends on the properties of vapor and membrane, i.e. the mean free path and mean pore size. However, in most cases, the models suggest that the mass flux may be written as a linear function of the vapor pressure difference across the membrane [3], given by:

$$J = C * (p_{m1} - p_{m2}) \quad (12)$$

Where J is the mass flux, C the membrane distillation coefficient, and p_{m1} and p_{m2} the partial pressure of water vapor at the membrane surfaces on the feed and permeate sides, respectively.

Equation (12), expressed previously, gives the mass flux (J) through the membrane as a function of the membrane mass transfer coefficient (C) and of the vapor pressure difference.

The membrane mass transfer coefficient (C) could be determined experimentally (semi-empirical model) [4] or theoretically (Knudsen model, molecular diffusion model and Hegan-Poiseuille viscous flow model) [5]. The vapor pressure can be calculated using Antoine's equation [6]:

$$p_v = \exp[B - \frac{A}{(D+T)}] \quad (13)$$

Where p_v is the vapor pressure in Pascal, T is the temperature in Kelvin, and A,B and D are experimental constants, (For water, A=3841, B=23.238 and D=-45).

Any decrease in the vapor pressure due to the salt concentration is calculated by Raoult's law, [6]:

$$\dot{p} = (1 - x_{ms}).p \quad (14)$$

Where p is the vapor pressure of pure water, $\dot{p}$ is the vapor pressure of the water with salt, and x_{ms} is the mole fraction of the salt at the membrane surface.

Since concentration polarization occurs, the mole fraction of the salt at the membrane surface is not the same as in the bulk. The salt concentration at the surface of the membrane could then be calculated using the film model [7],

$$C_{ms} = C_{bs}.\exp(\frac{J}{\rho.K_s}) \quad (15)$$

Where C_{ms} and C_{bs} are the salt concentration at the surface of the membrane and in the bulk respectively, ρ is the density of the bulk and K_s is the salt mass coefficient.

K_s could be evaluated by employing the Dittus-Boelter correlation by analog between heat transfer and mass transfer [8]:

For heat transfer:

$$Nu = 0.023 * Re^{0.83} * Pr^{0.33} = \frac{h.d_h}{k} \quad (16)$$

For mass transfer:

$$Sh = 0.023 * Re^{0.83} * Sc^{0.33} = \frac{K_s.d_h}{D_{wa}} \quad (17)$$

Where Sh is Shrood number, Sc is Schmidt number and d_h is the hydraulic diameter.

Schmidt number can be calculated from this equation:

$$Sc = \frac{\upsilon}{D_{wa}} = \frac{\mu}{\rho.D_{wa}} \quad (18)$$

Where υ is kinematic viscosity of water vapor, μ is dynamic viscosity of water vapor, ρ is density of water density and D_{wa} is diffusion coefficient of water vapor in stagnant air (m^2/s) estimated in eqn. (18).

Then, K_s can be calculated from the following equation:

$$K_s = 0.023 * Re^{0.83} * Sc^{0.33}.\frac{D_{wa}}{d_h}. \quad (19)$$

2.3 Performance Parameters

The two most commonly encountered performance metrics for solar desalination systems are the gained output ratio (GOR) of the desalination module and thermal efficiency of the system.

GOR is theoretical energy required to produce the distillate divided by the actual thermal energy consumed in the evaporator. Mathematically, the GOR of the membrane module can be written as [9],

$$GOR = \frac{\dot{m}_d * h_v}{\dot{m}_f.C_{p_f}*(T_{f_i}-T_{f_o})} \quad (20)$$

Where $\dot{m}_d$ is the distillate flow rate, $\dot{m}_f$ is the hot stream flow rate, and h_v is the latent heat of vaporization.

Efficiency of the system is the ratio between total latent heat in distilled water produced and the total input power to system. Mathematically, the η of the system can be written as:

$$\eta = \frac{\dot{m}_d.h_v}{W_{feed\ pump}+W_{cooling\ water\ pump}+Q_{Electric\ Heater}} \quad (21)$$

2.4 Method of Solving the Mathematical Model

For the calculation, a MATLAP program is written to solve the mathematical model. The model is divided into n segments and the water flux is computed iteratively for each segment Fig. 2. The exit cooling water temperature is first set at twenty degree Celsius and an iteration is then performed to calculate the permeate flux through the first segment.

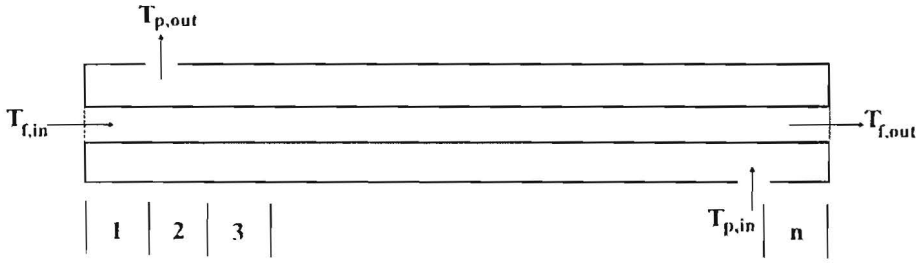

Fig. 2 Division of membrane module to n segments

The temperatures of the feed and of the cooling water are then calculated for the next segment by assuming that the total heat is transferred from the previous segment. At the last segment, the calculated cooling water temperature is compared with the actual one. If the difference is greater than the maximum acceptable difference, the calculation is repeated from the first segment with an updated cooling water temperature. The segment permeate fluxes are then added to give the total permeate flux through the membrane.

3. Experimental Procedure and Apparatus

Two membrane modules manufactured by Enka-Microdynn [10] were used. One was a hollow fiber "HF" unit for a theoretical model and the other a tubular membrane "TM" unit for both theoretical and experimental setup. The characteristics of the two units are summarized in Table 3.1. The experimental apparatus was almost the same for both membrane modules, Fig. 3. The only difference was the addition of a more powerful pump and of a bigger flow meter on the permeate side for the hollow fiber unit.

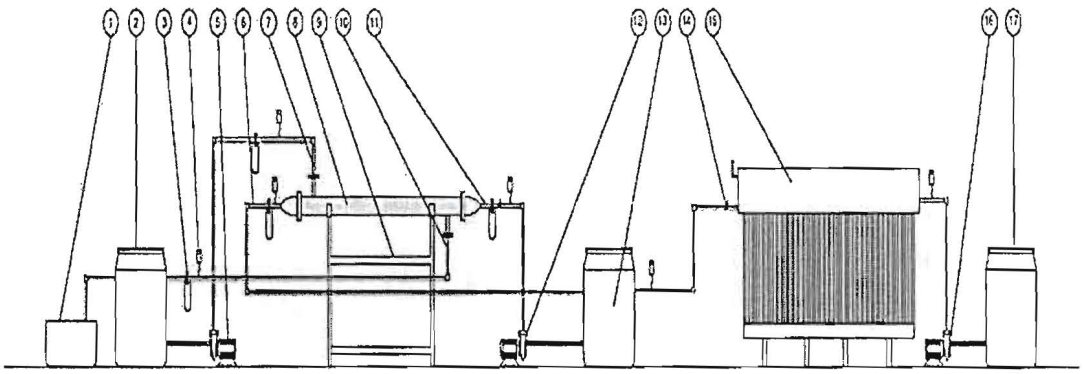

1. Permeate over flow tank.
2. Cooling water tank
3. Orfice meter
4. Thermocouple
5. Cooling water pump
6. Outlet feed water pipe
7. Inlet cooling water pipe
8. Tubular Direct Contact Membrane Module.
9. Membrane base
10. Outlet cooling water pipe
11. Inlet feed water pipe
12. Feed water pipe
13. Feed water tank
14. Manual valve
15. Water solar heater
16. Supply pump
17. Supply water tank

Fig. 3 Schematic of (DCMD) apparatus

The apparatus consists of two passes, feed water pass and cooling water pass. Feed water is heated in a vacuum tube water solar heater and salt is added to feed water in feed water tank before it pumped into tubular membrane by feed water pump. The apparatus is supplied with permeate over flow tank so that measurement of the permeation flux was easier and more accurate. This also enabled more convenient cleaning and prevention of micro-organism growth. For both passes, water flow rate was measured by orifice meters and controlled by a control valves. Temperature was measured by k-type thermocouples with temperature range of -200 to 1250 °C and special limits of error (above 0 °C) of 1.1 °C or 0.4%.

The experiments were carried out in the turbulent flow region for both feed and permeate sides. Feed water and cooling water flow rates in the range of 15 to 20 L/min. The feed water temperature was controlled at 70 °C by electric heater fixed in feed water tank, while cooling water temperature varied between 20 – 50 °C.

Feed solutions were pure water, aqueous NaCl solutions (10 gm NaCl / L water, 20 gm NaCl / L water, 30 gm NaCl / L water) and seawater (40 gm NaCl / L water).
For each case studied, permeate flow rate was measured every hour by orifice meter and total permeate water was collected and measured using permeate over flow tank

	Tubular membrane module "TM"	Hollow fiber membrane module "HFM"
Model type	MD 090 TP 2N ANSI	MD 080 CS 2N
Membrane area	1 m^2	2 m^2
Number of membranes	41	450
Nominal module diameter	9 cm	8 cm
Module length	1.5 m	1 m
Membrane inner diameter	5.5 mm	1.8 mm
Membrane outer diameter	8.5 mm	2.6 mm
Membrane thickness	1.5 mm	0.4 mm
Membrane porosity	75%	75%
Average pore size (determined by manufacturer)	0.2 μm	0.2 μm
Membrane material	Polypropylene	Polypropylene
Outer shell material	Polypropylene	Stainless Steel
Potting material	Polyurethane	Polyurethane

Table (1) Membrane unit characteristics

4. Result and discussion:

4.1 Effect of Feed Water Salt Concentration:-

Permeate flux decreases with an increase of salt concentration. This phenomenon can be attributed to the reduction of the driving force due to decrease of the vapor pressure of the feed solution and exponential increase of viscosity of feed water solution with increasing concentration. The contribution of concentration polarization effects is also known, however, this is very small compared with temperature polarization effect. As it is well known, MD can deal with feed solution with high concentrations without suffering the large drop in the permeability observed in other pressure-driven membrane processes.

As shown in Fig. 4, calculated permeate water flow rate of Tubular Membrane decreases by 7.33% due to changing salt concentration of water from pure water to 3g NaCl/L water solution, while productivity of pure water decreases by only 2.7% according to increasing of salt concentration from 3 to 50g Nacl/L water.

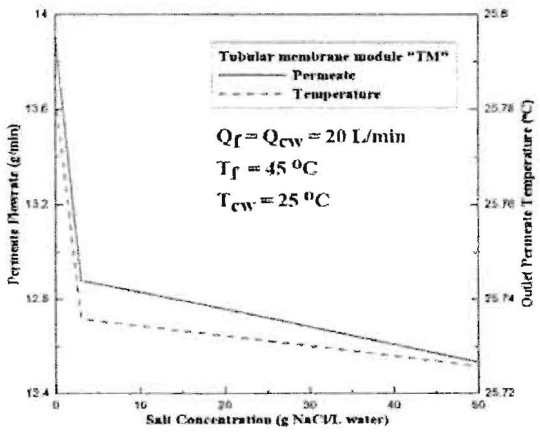

Fig. 4 Effect of salt concentration on TM performance

However, for Hollow Fiber Membrane as shown in Fig. 5 at the same conditions, pure water calculated productivity decreases by 20.48% due to increasing salt concentration from 0 to 3g NaCl/L water, while productivity of pure water decreases by only 3.6% due to increasing of salt concentration from 3 to 50 g NaCl/L water.

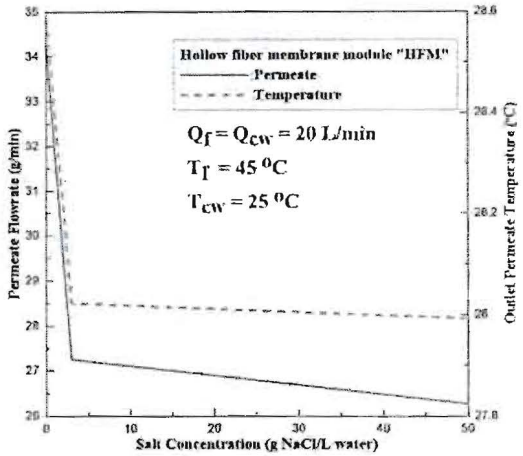

Fig. 5 Effect of salt concentration on HFM performance

For both Tubular and Hollow Fiber membranes, outlet permeate temperature is proportion to productivity of pure water and decreases a little with increasing of water salt concentration.

4.2 Effect of Feed Water Temperature

Various investigations have been carried out on the effect of feed water on permeate flux in MD. As shown in Fig. 6, it is clear that there is an exponential increase of permeate flow rate with the increase of feed temperature. As the driving force for membrane distillation is the difference in vapor pressure across the membrane, the increase of feed temperature increases the vapor pressure of feed solution, thus results in an increase in the transmembrane vapor pressure difference.

Although that increasing of feed temperature increases the driving force and so increases pure water productivity, feed temperature is limited at 70°C to avoid scale formation.

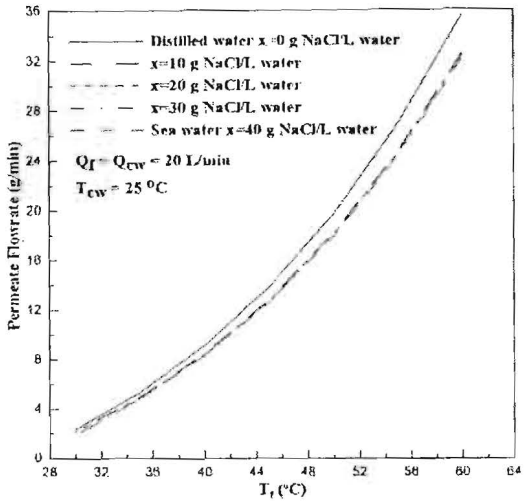

Fig. 6 Effect of feed water temperature on TM Productivity

4.3 Effect of Feed Water Flow rate

In MD, the increase of flow of the feed increases the permeate flow rate, the shearing force generated at high flow rate reduces the hydrodynamic boundary layer thickness and thus reduce polarization effect. Therefore, the temperature and concentration at the liquid-vapor interface becomes closer to corresponding values at the bulk of feed solution. Onsekizoglu et al. (2010) [11] studied the effects of various operating parameters on permeate flux and soluble solid content of apple juice during concentration through osmotic distillation (OD) and membrane distillation (MD) processes. They observed that the effect of feed flow rate on transmembrane flux was less than half of the influence of temperature difference across the membrane.

The effect of flow rate on MD flux becomes more noticeable at higher temperatures especially associated with higher temperature drop across the membrane [12]. Consequently, higher productivity can be achieved by operating under a turbulent flow regime. On the other hand, the liquid entry pressure of feed solution (LEP) must be taken into account in order to avoid membrane pore

wetting when optimizing feed flow rate [13, 14].

As shown in Figs. (7,8), for feed water flow rate between 15 and 20 L/min, the pure water permeate flow rate increases sharply.Thus because, in this region, feed water converts from laminar to tubular flow. So, in experimental work feed water flow rate is set after this region.

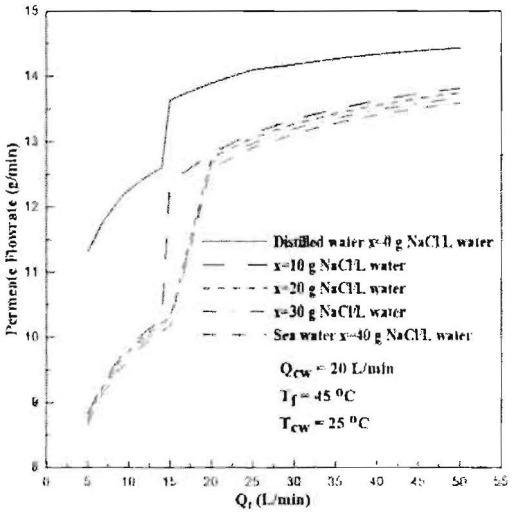

Fig. 7 Effect of feed water flow rate on Tubular Membrane

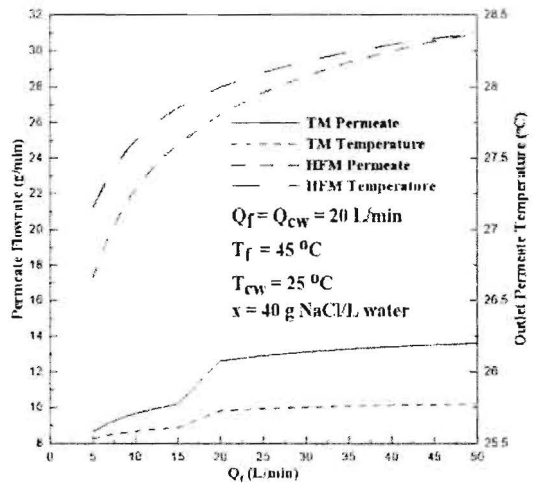

Fig. 8 Effect of feed water flow rate on Tubular and Hollow Fiber Membranes performance

4.4 Effect of Cooling Water Temperature

The increase of cooling water temperature results in lower MD productivity due to the decrease of the transmembrane vapor pressure difference as soon as the feed temperature is kept constant. It is noticed that the temperature of cold water in the permeate side has smaller effect on the permeate water productivity than that of the feed solution for the same temperature difference. This is because the vapor pressure increases exponentially with feed water.

As shown in Figs. 9,a,b,c,d and e, experimental work is performed at (T_{feed}= 70°C , feed water flowrate and cooling water flowrate both are set one time at 15 L/min and 20 L/min for other time. For Q_{feed}=$Q_{cooling\ water}$= 15L/min, temperature of cooling water increases from 20°C to 56°C. However, for Q_{feed}=$Q_{cooling\ water}$= 20 L/min, temperature of cooling water increases from 20°C to 50°C during 12hrs per day (from 7Am to 7Pm)) and salt concentration changes as shown in figures bellow from distilled water to x=40g NaCl/L water.

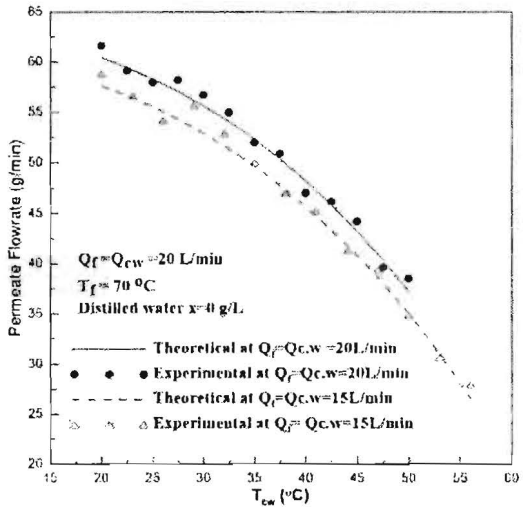

a- Distilled water (x=0g NaCl/ L water)

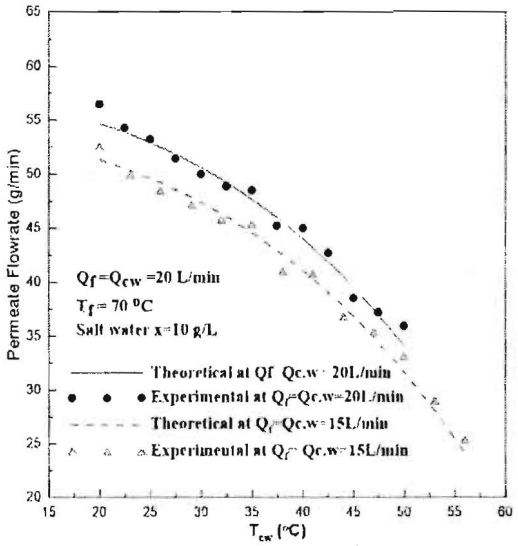

b- Salt water (x=10g NaCl/L water)

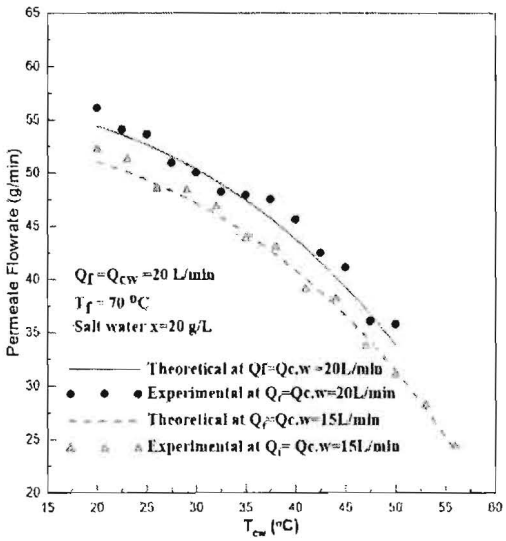

c. Salt water (x=20$_g$ Na Cl/ L water)

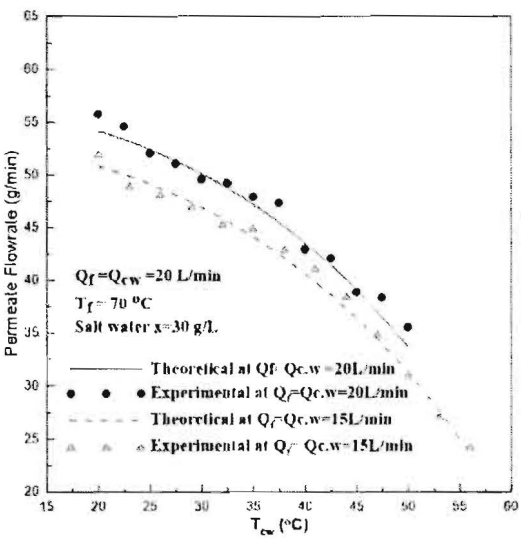

d. Salt water (x=30g NaCl/L water)

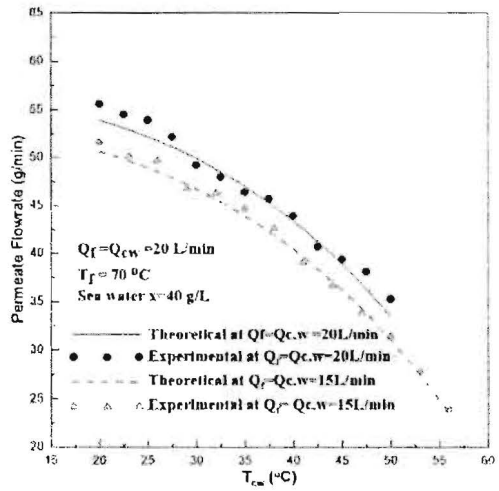

e. Sea Water (x= 40 g NaCl/L water)

Fig 9 Effect of cooling Water Temperature on TM Productivity

As shown in Figs. 8 (a,b,c,d and e), when salt concentration increases, pure water productivity decreases (for $Q_f = Q_{cw}$ =15L/min the pure water productivity decreases per day "12hrs" from 36.2148 kg/day to 31.8684 kg/day when salt concentration increases from 0g NaCl/L water to 40g NaCl/L water) and (for $Q_f = Q_{cw}$= 20L/min the pure water productivity decreases per day "12hrs" from 40.587kg/day to 37.0818kg/day when salt concentration increases from 0g NaCl/L water to 40g NaCl/L water).

5. Conclusion

The semi-empirical model used was the best at predicting the permeate flux. Its predictions are in very good agreement with the experimental values for both the hollow fiber and tubular units where the error is about 3-4%. Results showed that the amount of permeate water productivity increases strongly with the feed water flow rate and its inlet temperature and slightly decreases with its salt concentration. With the tubular module, increasing salt concentration from distilled water to 4 wt.% NaCl salt solution results in decreasing the permeate productivity by 8.2%. Also cooling water flow rate influences water extraction, however productivity decreases with increasing of cooling water temperature. Maximum productivity, daily efficiency, and Gain output ratio (GOR) reach 40.587 kg/day, 64.88%, and 0.624 respectively. Finally, a good agreement has been found between the present numerical results and experimental results.

Acknowledgements

This research is funded by Tanta University, Faculty of engineering. I thank supervisors committee. I also thank my parents and all my friends for their support.

Nomenclature

C_P	specific heat, J/kg.K
D	tube diameter, m
C	Membrane distillation coefficient, kg/s.m2.Pa
h	Average heat transfer coefficient, W/m2.K
J	Permeate flux per unit area of membrane, kg/sec.m2
k	thermal conductivity of fluid, W/m.K
L	length of membrane, m
M	Molecular mass (kg.mol-1)
$\dot{m}$	Mass flow rate, kg/s
Nu	Average Nusselt number, dimensionless
p	Pressure, pa
Pr	Prandtl number, Dimensionless
Q	Heat transfer rate, W
Re	Reynolds number, dimensionless
t	time, s
T	temperature, K

Greek Letters

ρ	Density of glass wool layer
η	efficiency (eta)
ε	Porosity of the membrane
δ	Thickness of the membrane, m
μ	Fluid dynamic viscosity, kg/m.s

Subscripts

F	feed water
c.w	cooling water
fm	membrane surface at feed side
pm	membrane surface at permeate side
M	membrane surface
b	buk
i	inlet
Out	outlet

Abbreviations

MD	Membrane Distillation
DCMD	Direct Contact Membrane Distillation
TM	Tubular Membrane Module
HFM	Hollow Fiber Membrane Module

References

[1] K. Hota, K. Kikuchi, I. Hayano, T. Okabe, T. Goto, S. Kimura and H. Ohya, Experiment on seawater

desalination by membrane distillation, Desalination, 78 (1990) 177-185.

[2] E.A. Mason, A.P Malinauskas, in: S.W. Churchill (Ed.), Gas Transport in Porous Media: The Dusty-Gas Model, Elsevier, Amsterdam, 1983.

[3] K.W. Lawson, D.R. Lloyd, Membrane distillation. II. Direct contact MD, J. Membr. Sci. 120 (1996) 123–133.

[4] TOMASZEWSKA, M., Concentration and Purification of Fluosilicic Acid by Membrane Distillation, Ind. Eng. Chem. Res., 39, 3038-3041, 2000.

[5] BURGOYNE, A., VAHDATI, M.M., Permeate Flux Modeling of Membrane Distillation, Filtration and Separation, 49, January- February 1999.

[6] J. Phattaranawik, R. Jiraratananon, Direct contact membrane distillation: effect of mass transfer on heat transfer, J. Membr. Sci. 188 (2001) 137–143.

[7] Dahiru U. Lawal, Atia E. Khalifa, "Theoretical and Statistical Models for Predicting Flux in Direct Contact Membrane Distillation", Journal of Engineering Research and Applications, August 2014, pp.124-135.

[8] M.A. Salehi, R. Rostamani, "Review of membrane distillation for the production of fresh water from saline water", 2013 JNAS Journal-2013-2-S3/1072-1075.

[9] Jaochim Koschikowski, Marcel Wieghaus, Matthias Romel, Solar thermal-driven desalination plants based on membrane distillation, Desalination 156 (2003) 295 – 304.

[10] Ludovic Plasse, "Desalination by membrane distillation a comparative study of tubular and hollow fiber membrane units", McGill University, Montreal (2000).

[11] Onsekizoglu, P., Bahceci, K. S. & Acar, J. (2010), "The use of factorial design for modeling membrane distillation". Journal of Membrane Science, 349, 225-230.

[12] Walton, J., Lu, H., Turner, C., Solis, S. & Hein, H. 2004. "Solar and waste heat desalination by membrane distillation". El Paso: College of Engineering University of Texas.

[13] He, K., Hwang, H. J., Woo, M. W. & Moon, I. S. (2011) Production of drinking water from saline water by direct contact membrane distillation (DCMD). Journal of Industrial and Engineering Chemistry, 17, 41-48.

[14] Khayet, A., Matsuura, T., Mengual, J. I. & Qtaishat, M. (2006) Design of novel direct contact membrane distillation membranes. Desalination, 192, 105-111.